

# DragScene: Interactive 3D Scene Editing with Single-view Drag Instructions

Chenghao Gu<sup>1</sup> Zhenzhe Li<sup>2</sup> Zhengqi Zhang<sup>3</sup> Yunpeng Bai<sup>4</sup> Shuzhao Xie<sup>1</sup>  
Zhi Wang<sup>\*1</sup>

<sup>1</sup>Shenzhen International Graduate School, Tsinghua University

<sup>2</sup>College of Artificial Intelligence, Xi'an Jiaotong University

<sup>3</sup>School of Software, Beihang University

<sup>4</sup>Department of Computer Science, The University of Texas at Austin

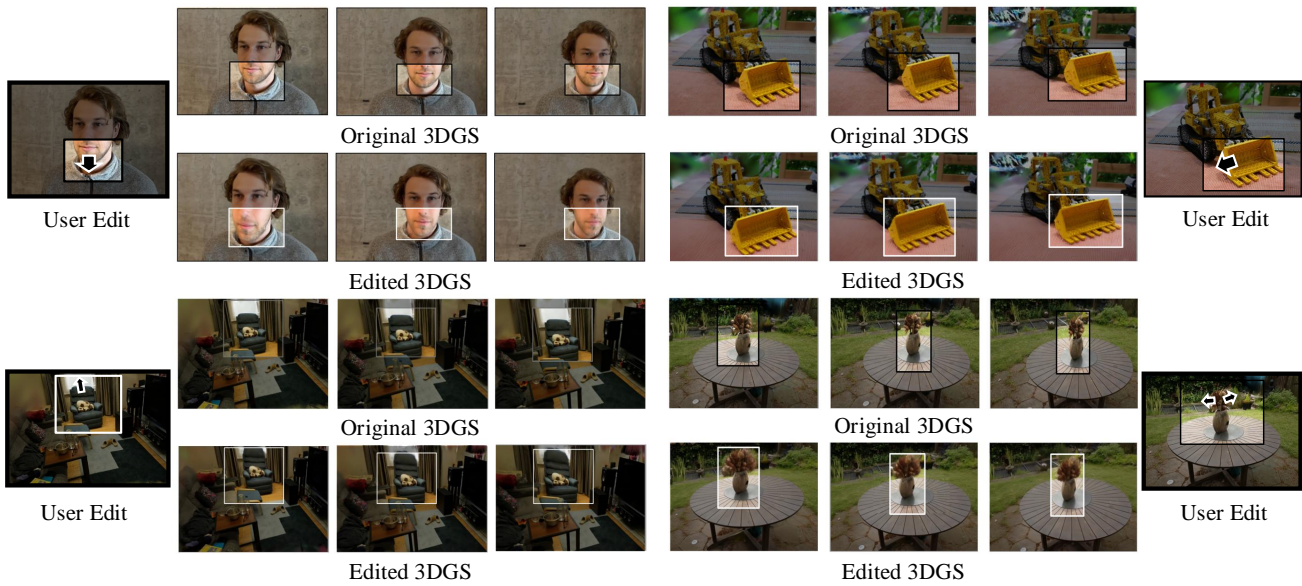


Figure 1. **Results of DragScene.** DragScene successfully enables drag-based editing for 3D scenes. By following user-provided editing instructions (masks and points), our model seamlessly performs drag-style editing on the original 3D scene. All the results presented above are based on 3D Gaussian Splatting (3DGS), demonstrating natural, creative, and view-consistent edits.

## Abstract

3D editing has shown remarkable capability in editing scenes based on various instructions. However, existing methods struggle with achieving intuitive, localized editing, such as selectively making flowers blossom. Drag-style editing has shown exceptional capability to edit images with direct manipulation instead of ambiguous text commands. Nevertheless, extending drag-based editing to 3D scenes presents substantial challenges due to multi-view inconsistency. To this end, we introduce DragScene, a framework that integrates drag-style editing with diverse 3D represen-

tations. First, latent optimization is performed on a reference view to generate 2D edits based on user instructions. Subsequently, coarse 3D clues are reconstructed from the reference view using a point-based representation to capture the geometric details of the edits. The latent representation of the edited view is then mapped to these 3D clues, guiding the latent optimization of other views. This process ensures that edits are propagated seamlessly across multiple views, maintaining multi-view consistency. Finally, the target 3D scene is reconstructed from the edited multi-view images. Extensive experiments demonstrate that DragScene facilitates precise and flexible drag-style editing of 3D scenes, supporting broad applicability across diverse 3D representations.

\* Corresponding author.

# 1. Introduction

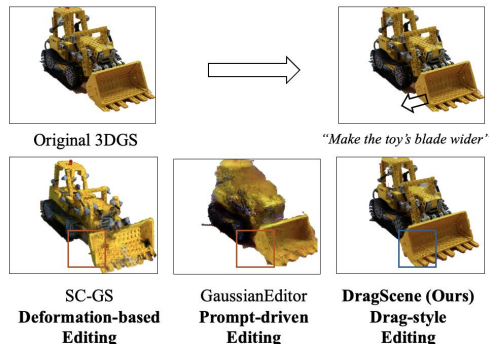
Recent advancements [23, 50] in technologies for reconstructing 3D scenes from the real world have become increasingly important across a wide range of applications. To effectively meet user needs, it is essential that these reconstructed scenes support precise and controllable modifications. Consequently, 3D editing techniques have garnered significant attention, providing new opportunities for interactive user experiences and customized adjustments.

Currently, many instruction-driven 3D editing methods offer excellent editing results, providing specific control over elements in a scene. Deformation-based editing methods [22, 46] are able to deform 3D objects with techniques such as cages. However, they fail to achieve creative and precise editing effects due to the limitations of simple shape deformation and the lack of support for rich visual priors. As illustrated in Fig. 2(a), we apply SC-GS [21] to perform the desired editing while producing unsatisfactory results.

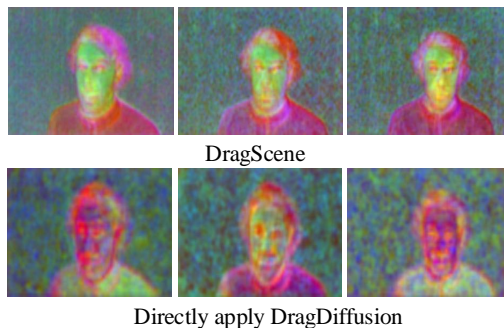
Prompt-driven methods, based on pre-trained 2D diffusion models [2, 36], can provide a wide variety of editing results based on text input, but are limited to overall appearance editing of the scene, lacking the ability of precise control over specific elements in the scene. The failure case conducted with GaussianEditor [42] in Fig. 2(a) shows the limitation of prompt-driven methods.

Nowadays, a novel drag-style image editing method pioneered by DragGAN [34] has garnered widespread attention, where users are enabled to provide instructions like “drag” to edit a 2D image interactively and obtain realistic and rich editing results. However, it is challenging to propagate the 2D drag-style editing method a 3D scenes while maintaining multi-view consistency. As shown in Fig. 2(b), we visualize the UNet feature maps [37] of multi-view images with principal component analysis (PCA) during the diffusion process when applying DragDiffusion [38] to multi-view images of 3D content. We observe that naively applying 2D drag-style editing to 3D scenes causes inconsistent features, leading to severe 3D discontinuities in editing.

To handle the aforementioned challenges, we introduce DragScene, a novel framework designed for flexible and controllable drag-based 3D editing while ensuring multi-view consistency. DragScene begins by rendering multi-view images of a 3D scene, and users are allowed to select a reference view to draw masks as editing regions and click handle points and target points to guide editing. Subsequently, we perform the desired editing on the reference view with 2D latent diffusion models, which optimize the latent of the original image to generate edits. To ensure consistent editing across multiple views, coarse point cloud representation of the edits is reconstructed as 3D clues to guide the further editing of other views. However, we observe that directly applying dense stereo methods to reconstruct the point cloud from a single edited image leads to significant deviations



(a) Existing methods fail to produce satisfactory edits for specific cases, while DragScene generates the desired edits with a simple 'drag' instruction.



(b) PCA visualization of UNet feature maps

Figure 2. **Our Motivation.** Comparison of DragScene and Directly applying DragDiffusion to multi-view images. (a) illustrates that existing 3D editing methods fail to solve the specific editing task and DragScene performs well. (b) PCA visualization of UNet feature maps during the diffusion process. It demonstrates that directly applying 2D drag-style methods to multi-view images produces inconsistent features, whereas DragScene maintains multi-view feature consistency throughout the diffusion process.

from the original scene. Therefore, we propose an effective optimization strategy for single-view point cloud reconstruction in the presence of scene edits, ensuring alignment with both the original scene and the edited region. To ensure consistency with the latent optimization process of the reference view, we assign the point cloud with the latent representation of the edited image. View-consistent latent maps can be rendered to further guide the latent optimization of other views, generating edited multi-view images with strong 3D consistency to reconstruct the final 3D representation of the edited scene. Extensive quantitative and qualitative experiments demonstrate that our method can achieve precise and creative editing results while maintaining excellent multi-view consistency.

To summarize, our contributions can be summarized as follows: 1) we propose an efficient 3D scene editing method named DragScene, which is the first drag-style 3D editing model applicable to real-world scenes. 2) we introduce a new mechanism to ensure multi-view consistency of 3D

editing, effectively mapping 2D edits to multi-view images. 3) comprehensive experiments validate the versatility and generality of DragScene, which is highly competitive with existing editing methods.

## 2. Related Work

### 2.1. 3D Scene Reconstruction

Our framework is based on learnable 3D representations for scene reconstruction, which enables high-quality reconstruction through the learning of multi-view image information. The first neural network-based model for 3D reconstruction, Neural Radiance Field (NeRF) [29], brings groundbreaking advancements to 3D reconstruction. NeRF and its variants [1, 4, 13, 15, 24, 32, 48] enable accurate learning accurate scene representation through multi-view images. 3D Gaussian Splatting (3DGS) [23] proposed in 2023 surpasses NeRF in both reconstruction quality and speed, setting a new trend. Follow-up work [20, 28, 41] continues to introduce more effective methods for 3D scene reconstruction.

### 2.2. 3D Scene Editing

3D editing methods allow users to modify the reconstructed scene according to specific editing requirements. Precise control over the appearance of a scene is achieved through two main methods: deformation-based methods and diffusion-based methods.

Deformation-based methods [7, 21, 25, 47, 50] leverage efficient techniques, such as cages [22, 35, 46], to deform the 3D representation into target positions, enabling edits like movement and reshaping. However, due to the inherent limitations of simple deformation, these methods often lack creativity and struggle to modify fine details.

Diffusion-based methods allow for a direct description of editing requirements to change the overall appearance of the original scene. Current methods [6, 8, 9, 12, 17, 22, 42, 44] leverage pre-trained 2D diffusion models [2, 36] to guide the update of the 3D representation. While these methods allow for flexible and realistic edits, they often lack the precision needed to target specific details, which highlights the importance of our DragScene.

### 2.3. Drag-style Editing

Drag-style editing allows users to make precise adjustments to specific elements within an image. DragGAN [34] enhances a pre-trained GAN [14] with feature-based motion supervision and point tracking for effective image editing. DragDiffusion [38] extends drag-style editing to the diffusion models and enables efficient spatial control by optimizing the latent during the diffusion process, while DragonDiffusion [31] improves consistency using feature correspondence and visual cross-attention. SDE-Drag [33] and Region-Drag [27] employ copying and pasting methods within the

diffusion latent space to achieve an efficient editing process.

Meanwhile, drag-style editing can be extended beyond images. Drag-based video editing methods [10, 40] effectively apply drag-style editing to videos, ensuring consistency across frames. MVDrag3D [5] enables drag-style editing for 3D objects, offering a flexible and creative 3D editing approach. Despite these advancements, extending drag-style editing to real 3D scenes with complex backgrounds and details remains a challenge. Our DragScene addresses these challenges with the powerful generative capabilities of diffusion models and 3D clues derived from point-based representations.

## 3. Methodology

In this section, we formally present the DragScene method. Given a reconstructed real-world 3D scene, users provide masks and pairs of dragging points on the reference view to perform editing across the entire 3D scene. Sec. 3.1 introduces the drag-style editing on the reference view and the acquisition of the reference latent representation. Sec. 3.2 outlines the consistent reconstruction of the latent representation, enabling editing operations that are tailored to multiple views. Sec. 3.3 discusses the specifics of latent optimization supervised by the reconstructed 3D latent maps for novel views. Finally, Sec. 3.4 details the reconstruction of the target 3D scene based on the edited view-consistent images.

### 3.1. Reference View Editing

Diffusion-based drag-style editing models focus on manipulating precise content editing for images, which is achieved by exerting controllable modifications to the latent representation during the diffusion process. In this paper, we employ DragDiffusion [38] as the editing method on the reference view due to its suitable latent optimization strategy and powerful editing ability.

As a preliminary step, drag instructions and mask  $M$  are provided by users according to the reference image  $I_0$  rendered from the original 3D scene. A DDIM inversion process [39] is applied on the image and obtain a diffusion latent  $\hat{z}_{t_e}^{(0)}$  at a certain step  $t_e$ . Through two steps namely Motion Supervision and Point Tracking, the diffusion latent is optimized through  $m$  steps to  $\hat{z}_{t_e}^{(m)}$ , and  $F(\hat{z}_{v_0, t_e}^{(k)})$  is the UNet output feature map. Also, two additional techniques, namely identity-preserving fine-tuning and reference-latent-control, are used to preserve the identity of the original scene. Following this, the image of the reference view is edited to the desired result  $\hat{I}_0$ .

We found that the latent representation obtained from the DragDiffusion process contains excessive noise, which makes it difficult to guide the subsequent optimization process. To derive a suitable representation in latent space, we perform an additional inversion process with a specific step

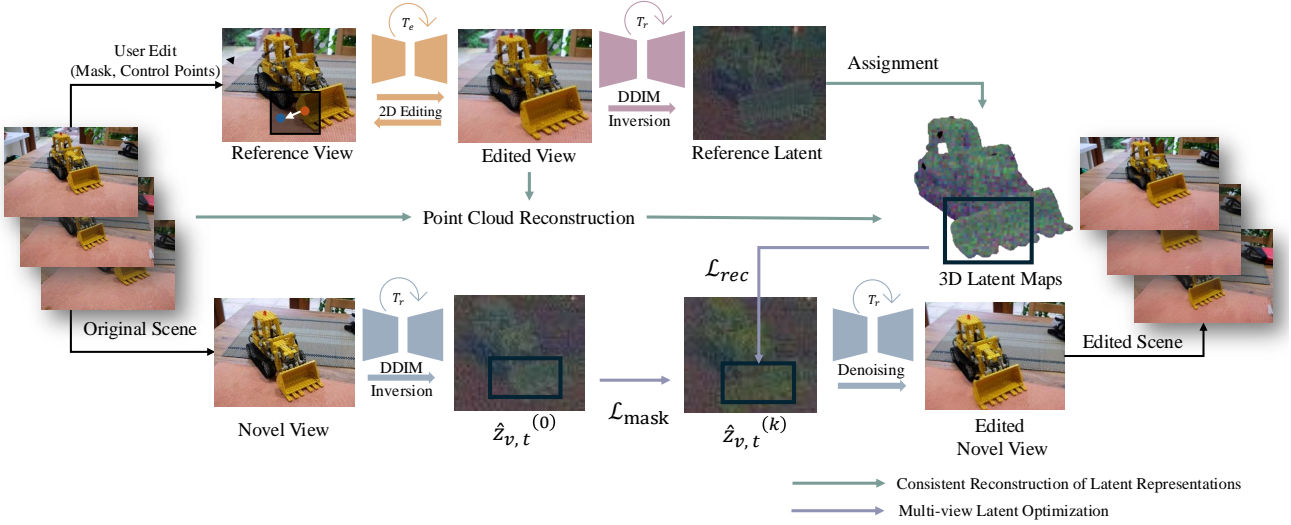


Figure 3. **Overview of DragScene.** Our approach consists of three steps: firstly, we apply a 2D drag-based diffusion model to edit the reference image and obtain the reference latent representation through DDIM inversion. Second, we perform consistent construction of the reference latent representation to obtain 3D latent maps. Finally, we apply the Inversion process to other views, further optimizing the images in latent space with the reconstructed 3D latent maps.

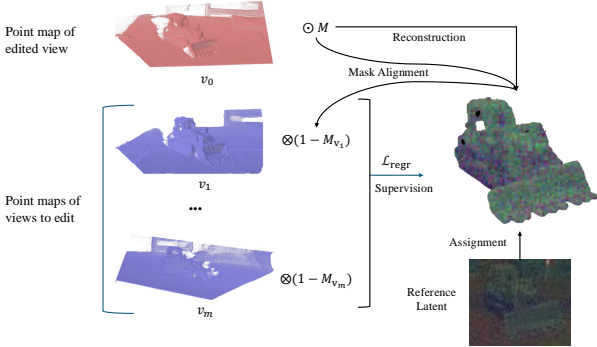


Figure 4. **Consistent Reconstruction of Latent Representations.** To facilitate consistent multi-view latent optimization, we apply DUST3R to reconstruct the coarse 3D point cloud, with aligned masks assisting in the optimization process. The latent representation of the reference image is assigned to the point cloud to obtain the 3D latent maps.

$t_r$  on the edited image to obtain the latent representation  $\hat{z}_{t_r}$ .

### 3.2. Consistent Reconstruction of Latent Representations

Before editing other views of the original scene, we perform a consistent reconstruction of latent representation based on the prior diffusion process. This module, as detailed in Fig. 4, ensures that the edits are propagated consistently across different views within the scene.

Initially, DUST3R [43] serves as the basic model to estimate the geometry information of the edits. To ensure that the coarse 3D clues of the edits do not deviate significantly from the original scene, we select the edited reference image  $I_0$  and a sparse set of original images from other views,

$\mathcal{I} = \{I_1, I_2, \dots, I_s\}$ , as the input.

During the point cloud reconstruction process, we obtain a set of pointmaps  $\{X_0, X_1, \dots, X_s\}$  based on the edited image  $I_0$  and the image set  $\mathcal{I}$ .  $X_{n,m}$  represents the pointmap  $X_n$  from view  $v_n$ , expressed in the coordinate frame of view  $v_m$ . To ensure consistency in the edited region, the mask  $M$  provided by the user in the reference view  $v_0$  is also transformed to view  $v_m$ . The transformation is as follows:

$$X_{n,m} = P_m P_n^{-1} h(X^n), \quad (1)$$

$$M_{v_m} = P_m P_0^{-1} h(M), \quad (2)$$

where  $P_m$  and  $P_n$  are the world-to-camera poses for images  $n$  and  $m$  respectively. The function  $h$  is a homogeneous mapping defined as  $h : (x, y, z) \rightarrow (x, y, z, 1)$ .

It needs to be ensured that the unmasked regions align with all views, while the masked regions align with the edits of the reference view. The regression loss for pixel  $i$  on view  $m$  is defined as follows:

$$\begin{aligned} \mathcal{L}_{regr}(m, i) = & \frac{1}{s+1} \sum_{n=0}^s \left\| \left( \frac{1}{z} X_i^m - \frac{1}{z} \bar{X}_i^{n,m} \right) \odot (1 - M_{v_m}) \right\| \\ & + \left\| \left( \frac{1}{z} X_i^m - \frac{1}{z} \bar{X}_i^{0,m} \right) \odot M_{v_m} \right\|, \end{aligned} \quad (3)$$

where  $\odot$  denotes the Hadamard product.

After reconstructing the coarse point cloud  $\mathcal{P}$ , we assign the latent representation  $\hat{z}_{t_r}$  and mask  $M$  to the point cloud to obtain the attributed point cloud  $P_{\mathcal{Z}}$  as the 3D latent

representation and  $P_{\mathcal{M}}$  as the 3D mask. For the set of views  $\mathcal{V} = \{v_1, v_2, \dots, v_s\}$  designated for editing, we can obtain consistent latent maps and editing masks through rendering, which serves to guide the subsequent latent optimization of other views.

### 3.3. Multi-View Latent Optimization

This section provides a detailed description of the multi-view latent optimization process in DragScene, which optimizes the image latent during the diffusion process with consistent latent representations and masks.

Inspired by the latent optimization in DragDiffusion [38], we first perform a DDIM inversion on the novel view image  $I_{v_i}$  to obtain the diffusion latent representation  $z_{v_i, t_r}$  at step  $t_r$ . We denote the initial latent representation as  $z_{v_i, t_r}^{(0)}$ . The latent map  $R_{v_i}(\mathcal{P}_{\mathcal{Z}})$  and the editing mask  $R_{v_i}(\mathcal{P}_{\mathcal{M}})$  are obtained through the rendering process  $R_{v_i}(\cdot)$  that projects the values of point cloud to image given view  $v_i$ .

The loss function at the  $k$ -th iteration is:

$$\mathcal{L}_{\text{total}} = \mathcal{L}_{\text{rec}} + \lambda \mathcal{L}_{\text{mask}}, \quad (4)$$

where

$$\mathcal{L}_{\text{rec}} = \left\| (z_{v_i, t_r}^{(0)} - \mathcal{S}_g(R_{v_i}(\mathcal{P}_{\mathcal{Z}}))) \odot R_{v_i}(\mathcal{P}_{\mathcal{M}}) \right\|_1, \quad (5)$$

and

$$\mathcal{L}_{\text{mask}} = \left\| (\hat{z}_{v_i, t_r}^{(k)} - \mathcal{S}_g(\hat{z}_{v_i, t_r}^{(0)})) \odot (1 - R_{v_i}(\mathcal{P}_{\mathcal{M}})) \right\|_1. \quad (6)$$

Here,  $\hat{z}_{v_i, t_r}^{(k)}$  represents the latent at the  $k$ -th iteration, and  $\mathcal{S}_g(\cdot)$  denotes the stop-gradient operator. In each iteration,  $\hat{z}_{v_i, t_r}^{(k)}$  is optimized by performing a single gradient descent step to minimize the total loss function  $\mathcal{L}_{\text{total}}$ :

$$\hat{z}_{v_i, t_r}^{(k+1)} = \hat{z}_{v_i, t_r}^{(k)} - \sigma \cdot \frac{\partial \mathcal{L}_{\text{total}}(\hat{z}_{v_i, t_r}^{(k)})}{\partial \hat{z}_{v_i, t_r}^{(k)}}, \quad (7)$$

where  $\sigma$  is the learning rate for latent optimization. During the optimization,  $\mathcal{L}_{\text{rec}}$  aligns the latent representation with the target latent map, while  $\mathcal{L}_{\text{mask}}$  constrains the unmasked regions to stay close to the original latent representation.

Then, we conduct the diffusion process  $f_{t_r \rightarrow 0}$  with the optimized latent representation  $\hat{z}_{v_i, t_r}^{(m)}$  after  $m$  iterations to obtain  $\hat{z}_{v_i, 0}$ . Then the edited image  $\hat{I}_{v_i}$  can be generated through decoding  $D(\hat{z}_{v_i, 0})$ .

### 3.4. Reconstruction of Edited Scenes

After finishing the multi-view consistency optimization, we employ these 2D views to edit the corresponding 3D scene. Here, we take 3D Gaussian Splatting (3DGS) [23] as an example due to its exceptional performance and speed in reconstructing unbounded scenes, and it has been widely adopted in a variety of applications [3, 26, 45, 51]. For the

original 3DGS scene, we define a set of camera poses to render a set of multi-view images of the scene. Then, the steps introduced above are conducted to generate consistent edited multi-view images, which are then used for further 3DGS reconstruction. DragScene successfully propagates the drag-style edits performed on the reference view to the whole 3D representation, generating the target 3D scene that adheres to the editing instructions.

DragScene is a general 3D scene editing method, not tied to one specific 3D representation. It achieves 3D-consistent editing solely based on image information, which gives significant potential for extensibility to newly emerged 3D reconstruction models.

## 4. Experiment

### 4.1. Implementation Details

To build our diffusion model, we adopt Stable Diffusion v1.5 [36] as the base model for the editing operation in DragScene. To enhance the multi-view consistency, we adopt the identity-preserving fine-tuning and reference latent control in DragDiffusion. We set the LoRA[19] rank to 16 and inject LoRA into the projection matrices of the query, key, and value tensors of every attention module. We then fine-tune LoRA with 80 iterations, using the AdamW optimizer[11] with a learning rate of  $5 \times 10^{-4}$ . During DDIM Inversion, we set the total number of steps  $t_{\text{total}}$  to 50, with  $t_e = 35$  and  $t_r = 20$ .

We base the implementation of 3DGS on Threestudio[16] and employ the optimized renderer from [23] for Gaussian rendering. For editing, we set a specific camera trajectory to capture the original image set with about 20 images for editing and reconstructing the edited scene based on the preset camera poses.

### 4.2. Experiment Setup

**Datasets** Recent advancements in drag-based editing techniques have highlighted a gap in available benchmark datasets, and several high-quality drag-style image editing datasets have recently emerged. However, a standardized dataset for evaluating drag-style edits in 3D scenes remains absent. To address this, we conduct our experiments on the Instruct-NeRF2NeRF [17] Dataset and Mip-NeRF 360 Dataset [1] which are mostly used in real-world 3D editing with various 3D scenes. To comprehensively assess the effectiveness of our method, we perform diverse editing operations on various objects within 3D scenes containing faces, scenery, furniture, and more.

**Baseline** As DragScene is the first method developed specifically for drag-style 3D scene editing, no universally recognized baselines exist for direct comparison. Therefore, to ensure an equitable comparison, we construct two comparative baselines. The first is GaussianEditor [42], a

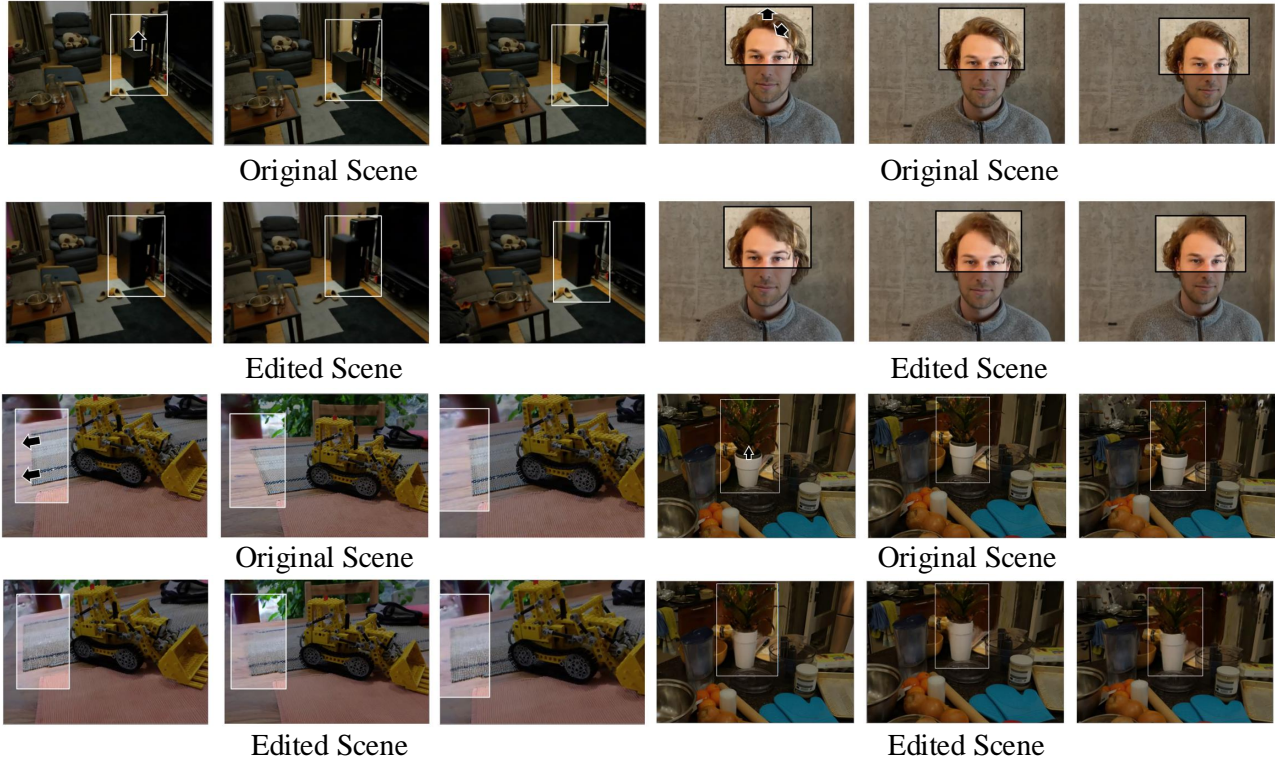


Figure 5. **More results of DragScene.** We present various views of both the original and edited scenes. All scenes are reconstructed using 3D Gaussian splatting.

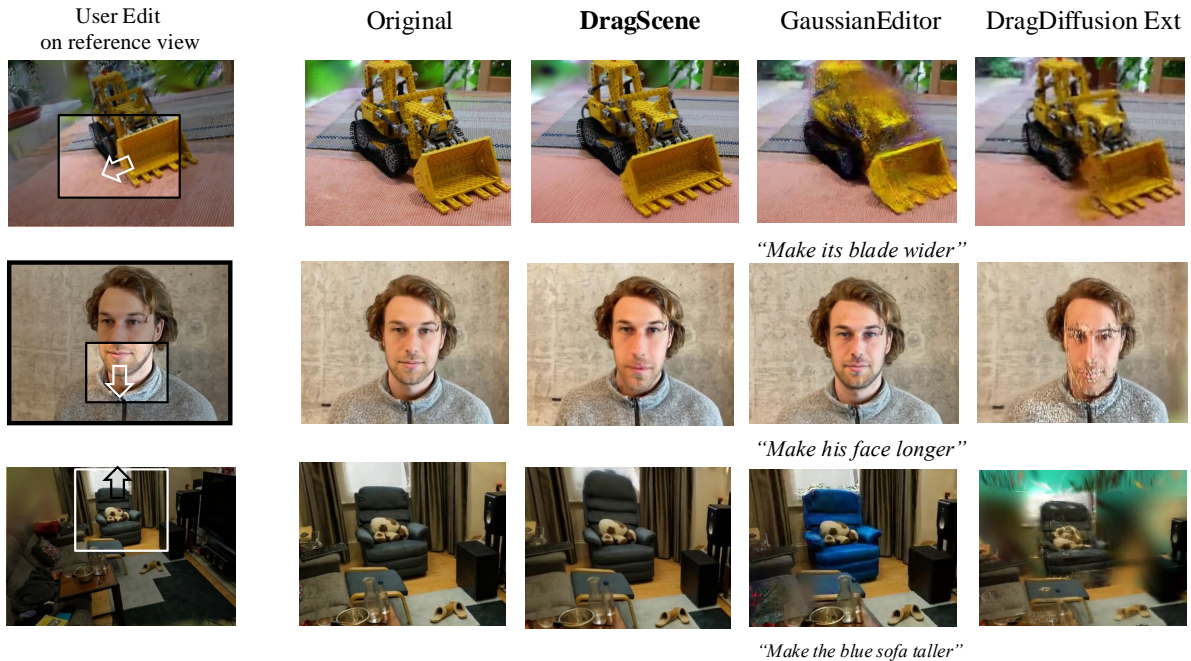


Figure 6. **Comparisons between DragScene and other methods.** We show the rendering view of scenes edited with different models. For fairness, we provide different forms of editing instructions with the same editing intent.

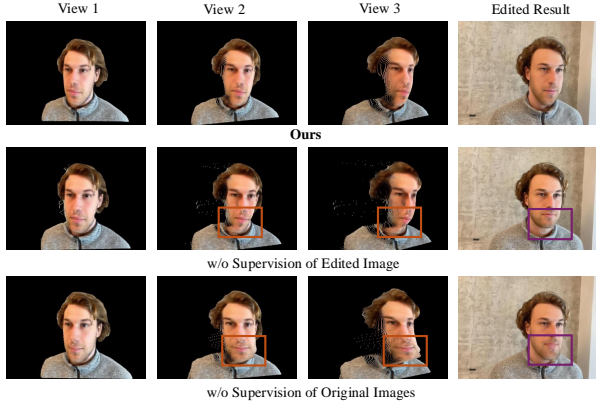


Figure 7. **Ablation on reconstruction of 3D clues.** The first three columns display the reconstructed point cloud of the reference view, and the fourth column shows the subsequent editing result. As shown, without the supervision of edited images, the predicted point cloud fails to accurately represent the target edited result, leading to mismatches in the latent features. Meanwhile, without the supervision of original images, the point cloud prediction deviates from the original scene. In contrast, DragScene’s point cloud reconstruction successfully generates accurate coarse 3D clues.

prompt-based 3D editing method, with carefully designed prompts to align with our targets. The second method applies DragDiffusion [38] directly on multi-view images, named DragDiffusion-3D extension. For fairness, we unify the 3D reconstruction for both DragScene and the baselines and the same drag instruction is applied.

### 4.3. Qualitative Evaluation

As shown in Fig. 5, our method surpasses other methods in both editing quality and controllability. Our framework demonstrates high-quality and precise editing capabilities in real-world 3D scenes, enabling users to achieve targeted editing effects with masks and control points provided from a single viewpoint. As we can see, the editing results are not limited to simple shape deformation and exhibit a broader range of complex generation. The edited scenes also exhibit excellent 3D consistency from multiple views and remain free from noticeable artifacts or failed reconstruction. Extensive examples highlight DragScene’s ability to effectively handle complex edits in 3D scenes, addressing limitations in other methods. Additional results can be found in the supplementary materials.

Meanwhile, we present a comparative analysis against other methods, as depicted in Fig. 6. It can be observed that the direct application of the DragDiffusion model to multi-view images leads to 3D inconsistencies and artifacts. Furthermore, compared to prompt-based editing techniques like GaussianEditor [42], it is clear that GaussianEditor fails to deliver satisfactory editing results based on the provided instructions. Moreover, Dragdiffusion-3D Extension suffers

from distortion and artifacts due to multi-view inconsistency.

### 4.4. Ablation on Reconstruction of 3D Clues

We conduct an ablation study on the reconstruction of 3D clues. During the optimization process of building a point cloud based on Dust3R, the edited reference image serves as the anchor view and the supervision of the original images is applied. The first row in Fig. 7 demonstrates that the coarse point cloud reconstruction method used in DragScene effectively preserves the original appearance of the scene.

When directly employing the 3D clues of the original scene (such as the original point cloud of 3DGS) instead of the newly generated point cloud from the edited image, incorrect region correspondence occurs during the point cloud assignment, due to the absence of the newly updated point cloud regions. For the example shown in the second row of Fig. 7, the mouth area in the original point cloud shifts toward the neck region after a drag operation, resulting in feature mismatches. Additionally, without supervision from the multi-view images of the original scene, the point cloud reconstructed using only the reference image exhibits distortions in unseen regions as shown in the third row of Fig. 7, resulting in discrepancies with the original scene.

### 4.5. Ablation Study on Inversion Process

We perform an ablation study to analyze the impact of the number of inversion steps  $t_r$  to optimize the latent of multi-view images. We schedule the number of total DDIM steps  $t_{total}$  to 50 and perform optimization at step  $t_r = t_{total} * \eta$ , where  $\eta$  is the inversion strength that controls the inversion process ( $\eta = 1$  indicates pure noise, and  $\eta = 0$  represents the original image).

As shown in Fig. 8, when  $\eta$  is relatively small, the noise in the latent representation is insufficient, resulting in lower image quality in the edited regions of the generated image. As  $\eta$  increases, the latent representation approaches noise, resulting in improved image quality. However, when  $\eta$  is too large, the result exhibits considerable deviation from the target and suffers from artifacts, which may cause inconsistencies across multiple views. It is evident that when  $\eta$  is around 0.4, the generated image achieves optimal quality, with the content closely matching the editing target.

Subsequently, we evaluate the quality and consistency of the generated images from novel viewpoints by taking the edited view as a reference. Since there is no ground truth for evaluation, we use a no-reference image quality metric named NIQE Score [30] to assess the quality of the generated images. Additionally, we calculate the FID score [18] between the generated images on the novel views and the edited reference view image to assess the degree of deviation from the editing target. As shown in Fig. 7, the optimal results are achieved when  $\eta$  is around 0.4.

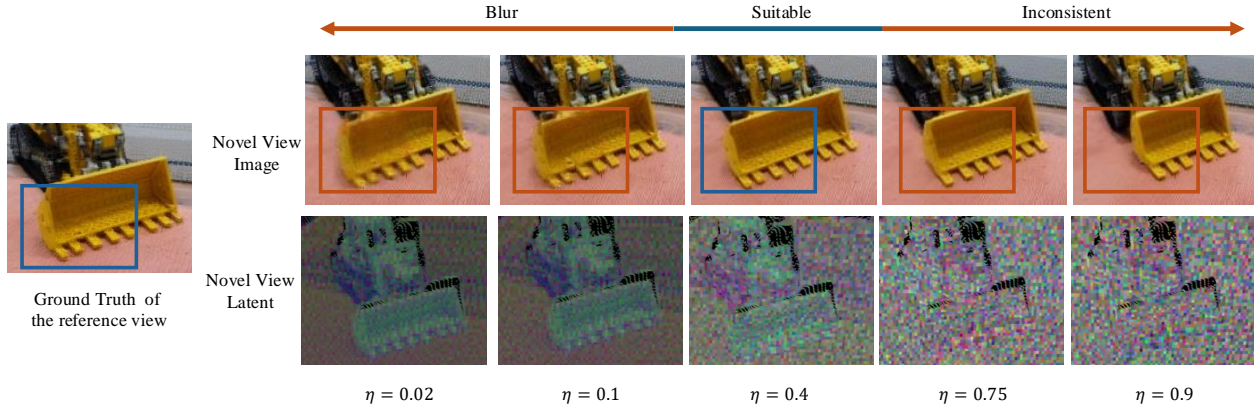


Figure 8. **Ablation Study on the the Inversion Strength**  $\eta = t_{opt}/t_{total}$ . Results of high quality and multi-view consistency are obtained when  $\eta$  is around 0.4. When the value of  $\eta$  is smaller, the noise in the latent representation decreases, leading to a more blurred output after optimization. On the other hand, when  $\eta$  is larger, the noise in latent representation increases, causing a greater deviation from the target result and the emergence of artifacts. When  $\eta$  is around 0.4, the quality of the optimized result is higher and closer to the target outcome.

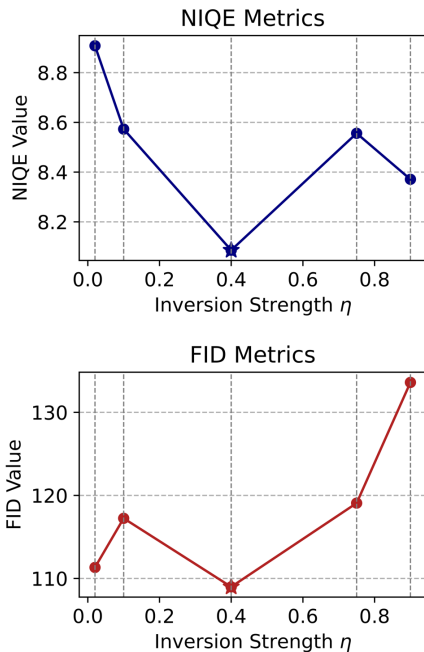


Figure 9. **Ablation study on the Inversion strength**  $\eta$ . NIQE Score ( $\downarrow$ ) and FID Score ( $\downarrow$ ) are reported. When the inversion strength  $\eta$  reaches 0.4, both metrics achieve their optimal performance.

## 5. Conclusion

In our research, we introduce DragScene, a novel 3D editing method that harnesses the powerful generative capabilities of diffusion models and the coarse 3D clues provided by point-based representations. Our work propose a novel

3D editing paradigm that effectively overcomes the limitations of previous methods and resolves the challenge of multi-view inconsistency in 3D editing. Users are allowed to perform controllable edits on complex 3D scenes interactively through simple editing instructions. DragScene enables flexible and creative drag-style editing on diverse 3D scenes while maintaining high fidelity and multi-view consistency. We hope that DragScene will inspire exciting new applications and drive innovative research to develop more user-friendly methods for 3D editing.

**Limitation.** Despite the advantages of our method, there are still several limitations to consider. Firstly, the effectiveness of editing is limited to the performance of 2D diffusion models when performing drag-based editing on the reference image. For example, DragDiffusion [38] may fail in some cases, such as opening the mouth of a man. Further research is encouraged to extend DragScene to support a broader range of 2D drag-based editing models. Meanwhile, the method may produce unsatisfactory results when the view range is too large, due to a lack of sufficient 3D clues. This issue is similar to that identified in other works such as [49] which also rely on coarse 3D clues to guide generation.

**Future Work.** In the future, additional research directions worth research. First, one promising direction for DragScene is to leverage large language models to use text prompt to guide drag instructions for 3D scene editing, enabling more user-friendly editing. Moreover, the editing method for static scenes can be further extended to dynamic scenes, allowing for controllable editing of more complex scenes. Furthermore, more editing paradigms can be explored based on the framework of our method, enabling more efficient editing on 3D scenes.



## References

- [1] Jonathan T Barron, Ben Mildenhall, Dor Verbin, Pratul P Srinivasan, and Peter Hedman. Mip-nerf 360: Unbounded anti-aliased neural radiance fields. In *Proceedings of the IEEE/CVF conference on computer vision and pattern recognition*, pages 5470–5479, 2022. 3, 5
- [2] Tim Brooks, Aleksander Holynski, and Alexei A Efros. Instructpix2pix: Learning to follow image editing instructions. In *Proceedings of the IEEE/CVF Conference on Computer Vision and Pattern Recognition*, pages 18392–18402, 2023. 2, 3
- [3] David Charatan, Sizhe Li, Andrea Tagliasacchi, and Vincent Sitzmann. pixelsplat: 3d gaussian splats from image pairs for scalable generalizable 3d reconstruction. In *CVPR*, 2023. 5
- [4] Anpei Chen, Zexiang Xu, Fuqiang Zhao, Xiaoshuai Zhang, Fanbo Xiang, Jingyi Yu, and Hao Su. Mvsnerf: Fast generalizable radiance field reconstruction from multi-view stereo. In *Proceedings of the IEEE/CVF international conference on computer vision*, pages 14124–14133, 2021. 3
- [5] Honghua Chen, Yushi Lan, Yongwei Chen, Yifan Zhou, and Xingang Pan. Mvdrag3d: Drag-based creative 3d editing via multi-view generation-reconstruction priors. *arXiv preprint arXiv:2410.16272*, 2024. 3
- [6] Jun-Kun Chen and Yu-Xiong Wang. Proedit: Simple progression is all you need for high-quality 3d scene editing. *arXiv preprint arXiv:2411.05006*, 2024. 3
- [7] Jun-Kun Chen, Jipeng Lyu, and Yu-Xiong Wang. Neuraleditor: Editing neural radiance fields via manipulating point clouds. In *Proceedings of the IEEE/CVF Conference on Computer Vision and Pattern Recognition*, pages 12439–12448, 2023. 3
- [8] Jun-Kun Chen, Samuel Rota Bulò, Norman Müller, Lorenzo Porzi, Peter Kotschieder, and Yu-Xiong Wang. Consistdreamer: 3d-consistent 2d diffusion for high-fidelity scene editing. In *Proceedings of the IEEE/CVF Conference on Computer Vision and Pattern Recognition*, pages 21071–21080, 2024. 3
- [9] Minghao Chen, Iro Laina, and Andrea Vedaldi. Dge: Direct gaussian 3d editing by consistent multi-view editing. *arXiv preprint arXiv:2404.18929*, 2024. 3
- [10] Yufan Deng, Ruida Wang, Yuhao Zhang, Yu-Wing Tai, and Chi-Keung Tang. Dragvideo: Interactive drag-style video editing. In *European Conference on Computer Vision*, pages 183–199. Springer, 2025. 3
- [11] P Kingma Diederik. Adam: A method for stochastic optimization. (*No Title*), 2014. 5
- [12] Jiahua Dong and Yu-Xiong Wang. Vica-nerf: View-consistency-aware 3d editing of neural radiance fields. *Advances in Neural Information Processing Systems*, 36, 2024. 3
- [13] Sara Fridovich-Keil, Alex Yu, Matthew Tancik, Qinhong Chen, Benjamin Recht, and Angjoo Kanazawa. Plenoxels: Radiance fields without neural networks. In *Proceedings of the IEEE/CVF conference on computer vision and pattern recognition*, pages 5501–5510, 2022. 3
- [14] Ian Goodfellow, Jean Pouget-Abadie, Mehdi Mirza, Bing Xu, David Warde-Farley, Sherjil Ozair, Aaron Courville, and Yoshua Bengio. Generative adversarial networks. *Communications of the ACM*, 63(11):139–144, 2020. 3
- [15] Yuan-Chen Guo, Di Kang, Linchao Bao, Yu He, and Song-Hai Zhang. Nerfren: Neural radiance fields with reflections. In *Proceedings of the IEEE/CVF Conference on Computer Vision and Pattern Recognition*, pages 18409–18418, 2022. 3
- [16] Yuan-Chen Guo, Ying-Tian Liu, Ruizhi Shao, Christian Laforte, Vikram Voleti, Guan Luo, Chia-Hao Chen, Zi-Xin Zou, Chen Wang, Yan-Pei Cao, and Song-Hai Zhang. threestudio: A unified framework for 3d content generation. <https://github.com/threestudio-project/threestudio>, 2023. 5
- [17] Ayaan Haque, Matthew Tancik, Alexei A Efros, Aleksander Holynski, and Angjoo Kanazawa. Instruct-nerf2nerf: Editing 3d scenes with instructions. In *Proceedings of the IEEE/CVF International Conference on Computer Vision*, pages 19740–19750, 2023. 3, 5
- [18] Martin Heusel, Hubert Ramsauer, Thomas Unterthiner, Bernhard Nessler, and Sepp Hochreiter. Gans trained by a two time-scale update rule converge to a local nash equilibrium. *Advances in neural information processing systems*, 30, 2017. 7
- [19] Edward J Hu, Yelong Shen, Phillip Wallis, Zeyuan Allen-Zhu, Yuanzhi Li, Shean Wang, Lu Wang, and Weizhu Chen. Lora: Low-rank adaptation of large language models. *arXiv preprint arXiv:2106.09685*, 2021. 5
- [20] Binbin Huang, Zehao Yu, Anpei Chen, Andreas Geiger, and Shenghua Gao. 2d gaussian splatting for geometrically accurate radiance fields. In *ACM SIGGRAPH 2024 Conference Papers*, pages 1–11, 2024. 3
- [21] Yi-Hua Huang, Yang-Tian Sun, Ziyi Yang, Xiaoyang Lyu, Yan-Pei Cao, and Xiaojuan Qi. Sc-gs: Sparse-controlled gaussian splatting for editable dynamic scenes. In *Proceedings of the IEEE/CVF Conference on Computer Vision and Pattern Recognition*, pages 4220–4230, 2024. 2, 3
- [22] Clément Jambon, Bernhard Kerbl, Georgios Kopanas, Stavros Diolatzis, Thomas Leimkühler, and George Drettakis. Nerf-shop: Interactive editing of neural radiance fields. *Proceedings of the ACM on Computer Graphics and Interactive Techniques*, 6(1), 2023. 2, 3
- [23] Bernhard Kerbl, Georgios Kopanas, Thomas Leimkühler, and George Drettakis. 3d gaussian splatting for real-time radiance field rendering. *ACM Trans. Graph.*, 42(4):139–1, 2023. 2, 3, 5
- [24] Lingjie Liu, Jiatao Gu, Kyaw Zaw Lin, Tat-Seng Chua, and Christian Theobalt. Neural sparse voxel fields. *Advances in Neural Information Processing Systems*, 33:15651–15663, 2020. 3
- [25] Steven Liu, Xiuming Zhang, Zhoutong Zhang, Richard Zhang, Jun-Yan Zhu, and Bryan Russell. Editing conditional radiance fields. In *Proceedings of the IEEE/CVF international conference on computer vision*, pages 5773–5783, 2021. 3
- [26] Guanxing Lu, Shiyi Zhang, Ziwei Wang, Changliu Liu, Jiwen Lu, and Yansong Tang. Manigaussian: Dynamic gaussian splatting for multi-task robotic manipulation. In *European Conference on Computer Vision*. Springer, 2024. 5

- [27] Jingyi Lu, Xinghui Li, and Kai Han. Regiondrag: Fast region-based image editing with diffusion models. *arXiv preprint arXiv:2407.18247*, 2024. 3
- [28] Xiaoyang Lyu, Yang-Tian Sun, Yi-Hua Huang, Xiuzhe Wu, Ziyi Yang, Yilun Chen, Jiangmiao Pang, and Xiaojuan Qi. 3dgsr: Implicit surface reconstruction with 3d gaussian splatting. *arXiv preprint arXiv:2404.00409*, 2024. 3
- [29] Ben Mildenhall, Pratul P Srinivasan, Matthew Tancik, Jonathan T Barron, Ravi Ramamoorthi, and Ren Ng. Nerf: Representing scenes as neural radiance fields for view synthesis. *Communications of the ACM*, 65(1):99–106, 2021. 3
- [30] Anish Mittal, Rajiv Soundararajan, and Alan C Bovik. Making a “completely blind” image quality analyzer. *IEEE Signal processing letters*, 20(3):209–212, 2012. 7
- [31] Chong Mou, Xintao Wang, Jiechong Song, Ying Shan, and Jian Zhang. Dragondiffusion: Enabling drag-style manipulation on diffusion models. *arXiv preprint arXiv:2307.02421*, 2023. 3
- [32] Thomas Müller, Alex Evans, Christoph Schied, and Alexander Keller. Instant neural graphics primitives with a multi-resolution hash encoding. *ACM transactions on graphics (TOG)*, 41(4):1–15, 2022. 3
- [33] Shen Nie, Hanzhong Allan Guo, Cheng Lu, Yuhao Zhou, Chenyu Zheng, and Chongxuan Li. The blessing of randomness: Sde beats ode in general diffusion-based image editing. *arXiv preprint arXiv:2311.01410*, 2023. 3
- [34] Xingang Pan, Ayush Tewari, Thomas Leimkühler, Lingjie Liu, Abhimitra Meka, and Christian Theobalt. Drag your gan: Interactive point-based manipulation on the generative image manifold. In *ACM SIGGRAPH 2023 Conference Proceedings*, pages 1–11, 2023. 2, 3
- [35] Yicong Peng, Yichao Yan, Shengqi Liu, Yuhao Cheng, Shanyan Guan, Bowen Pan, Guangtao Zhai, and Xiaokang Yang. Cagenerf: Cage-based neural radiance field for generalized 3d deformation and animation. *Advances in Neural Information Processing Systems*, 35:31402–31415, 2022. 3
- [36] Robin Rombach, Andreas Blattmann, Dominik Lorenz, Patrick Esser, and Björn Ommer. High-resolution image synthesis with latent diffusion models. In *Proceedings of the IEEE/CVF conference on computer vision and pattern recognition*, pages 10684–10695, 2022. 2, 3, 5
- [37] Olaf Ronneberger, Philipp Fischer, and Thomas Brox. U-net: Convolutional networks for biomedical image segmentation. In *Medical image computing and computer-assisted intervention—MICCAI 2015: 18th international conference, Munich, Germany, October 5-9, 2015, proceedings, part III 18*, pages 234–241. Springer, 2015. 2
- [38] Yujun Shi, Chuhui Xue, Jun Hao Liew, Jiachun Pan, Han-shu Yan, Wenqing Zhang, Vincent YF Tan, and Song Bai. Dragdiffusion: Harnessing diffusion models for interactive point-based image editing. In *Proceedings of the IEEE/CVF Conference on Computer Vision and Pattern Recognition*, pages 8839–8849, 2024. 2, 3, 5, 7, 8
- [39] Jiaming Song, Chenlin Meng, and Stefano Ermon. Denoising diffusion implicit models. *arXiv preprint arXiv:2010.02502*, 2020. 3
- [40] Yao Teng, Enze Xie, Yue Wu, Haoyu Han, Zhenguo Li, and Xihui Liu. Drag-a-video: Non-rigid video editing with point-based interaction. *arXiv preprint arXiv:2312.02936*, 2023. 3
- [41] Matias Turkulainen, Xuqian Ren, Iaroslav Melekhov, Otto Seiskari, Esa Rahtu, and Juho Kannala. Dn-splatter: Depth and normal priors for gaussian splatting and meshing. *arXiv preprint arXiv:2403.17822*, 2024. 3
- [42] Junjie Wang, Jiemin Fang, Xiaopeng Zhang, Lingxi Xie, and Qi Tian. Gaussianeditor: Editing 3d gaussians delicately with text instructions. In *Proceedings of the IEEE/CVF Conference on Computer Vision and Pattern Recognition*, pages 20902–20911, 2024. 2, 3, 5, 7
- [43] Shuzhe Wang, Vincent Leroy, Yohann Cabon, Boris Chidlovskii, and Jerome Revaud. Dust3r: Geometric 3d vision made easy. In *Proceedings of the IEEE/CVF Conference on Computer Vision and Pattern Recognition*, pages 20697–20709, 2024. 4
- [44] Yuxuan Wang, Xuanyu Yi, Zike Wu, Na Zhao, Long Chen, and Hanwang Zhang. View-consistent 3d editing with gaussian splatting. In *European Conference on Computer Vision*, pages 404–420. Springer, 2025. 3
- [45] Shuzhao Xie, Weixiang Zhang, Chen Tang, Yunpeng Bai, Rongwei Lu, Shijia Ge, and Zhi Wang. Mesongs: Post-training compression of 3d gaussians via efficient attribute transformation. In *European Conference on Computer Vision*. Springer, 2024. 5
- [46] Tianhan Xu and Tatsuya Harada. Deforming radiance fields with cages. In *European Conference on Computer Vision*, pages 159–175. Springer, 2022. 2, 3
- [47] Bangbang Yang, Chong Bao, Junyi Zeng, Hujun Bao, Yinda Zhang, Zhaopeng Cui, and Guofeng Zhang. Neumesh: Learning disentangled neural mesh-based implicit field for geometry and texture editing. In *European Conference on Computer Vision*, pages 597–614. Springer, 2022. 3
- [48] Alex Yu, Ruilong Li, Matthew Tancik, Hao Li, Ren Ng, and Angjoo Kanazawa. Plenotrees for real-time rendering of neural radiance fields. In *Proceedings of the IEEE/CVF International Conference on Computer Vision*, pages 5752–5761, 2021. 3
- [49] Wangbo Yu, Jinbo Xing, Li Yuan, Wenbo Hu, Xiaoyu Li, Zhipeng Huang, Xiangjun Gao, Tien-Tsin Wong, Ying Shan, and Yonghong Tian. Viewcrafter: Taming video diffusion models for high-fidelity novel view synthesis. *arXiv preprint arXiv:2409.02048*, 2024. 8
- [50] Yu-Jie Yuan, Yang-Tian Sun, Yu-Kun Lai, Yuewen Ma, Rongfei Jia, and Lin Gao. Nerf-editing: geometry editing of neural radiance fields. In *Proceedings of the IEEE/CVF Conference on Computer Vision and Pattern Recognition*, pages 18353–18364, 2022. 2, 3
- [51] Xiaoyu Zhou, Zhiwei Lin, Xiaojun Shan, Yongtao Wang, Deqing Sun, and Ming-Hsuan Yang. Drivinggaussian: Composite gaussian splatting for surrounding dynamic autonomous driving scenes. In *Proceedings of the IEEE/CVF Conference on Computer Vision and Pattern Recognition*, pages 21634–21643, 2024. 5